

Supporting Information for

**Ni(II)-Based Metallasupramolecular
Polymer with Carboxylic Acid Groups: A
Stable Platform for Smooth Imidazole
Loading and the Anhydrous Proton
Channels Formation**

*Yemineni S L V Narayana, Takefumi Yoshida, Manas Kumar Bera, Sanjoy Mondal, and
Masayoshi Higuchi**

Electronic Functional Macromolecules Group, National Institute for Materials Science
(NIMS), Tsukuba 305-0044, Japan, Email: HIGUCHI.Masayoshi@nims.go.jp

Contents

- 1. ^1H NMR, MALDI-TOF and FT-IR spectra of compound 3**
- 2. ^1H NMR, MALDI-TOF and FT-IR spectra of ligand (L)**
- 3. XANFS data of polyNi**
- 4. XPS data of polyNi**
- 5. Derivative TG plot of polyNi-Im**
- 6. FT-IR analysis of imidazole, polyNi, and polyNi-Im**
- 7. MALDI-TOF analysis of polyNi and polyNi-Im**
- 8. SEM images of polyNi and polyNi-Im**
- 9. FESEM-EDX analysis of polyNi and polyNi-Im powder and the assembled states**
- 10. Proton conductivity data of polyNi under anhydrous conditions**
- 11. TGA data of polyNi-Im before and after the impedance measurement**
- 12. Powder XRD data of polyNi-Im before and after the impedance measurement**
- 13. Bode plot of polyNi-Im at 120 °C**
- 14. Nyquist plot of polyNi-Im at 120 °C**
- 15. Comparison of proton conductivity of polyNi-Im at 120 °C with different kinds of imidazole loaded materials**

1. ^1H NMR, MALDI-TOF and FT-IR Spectra of Compound 3

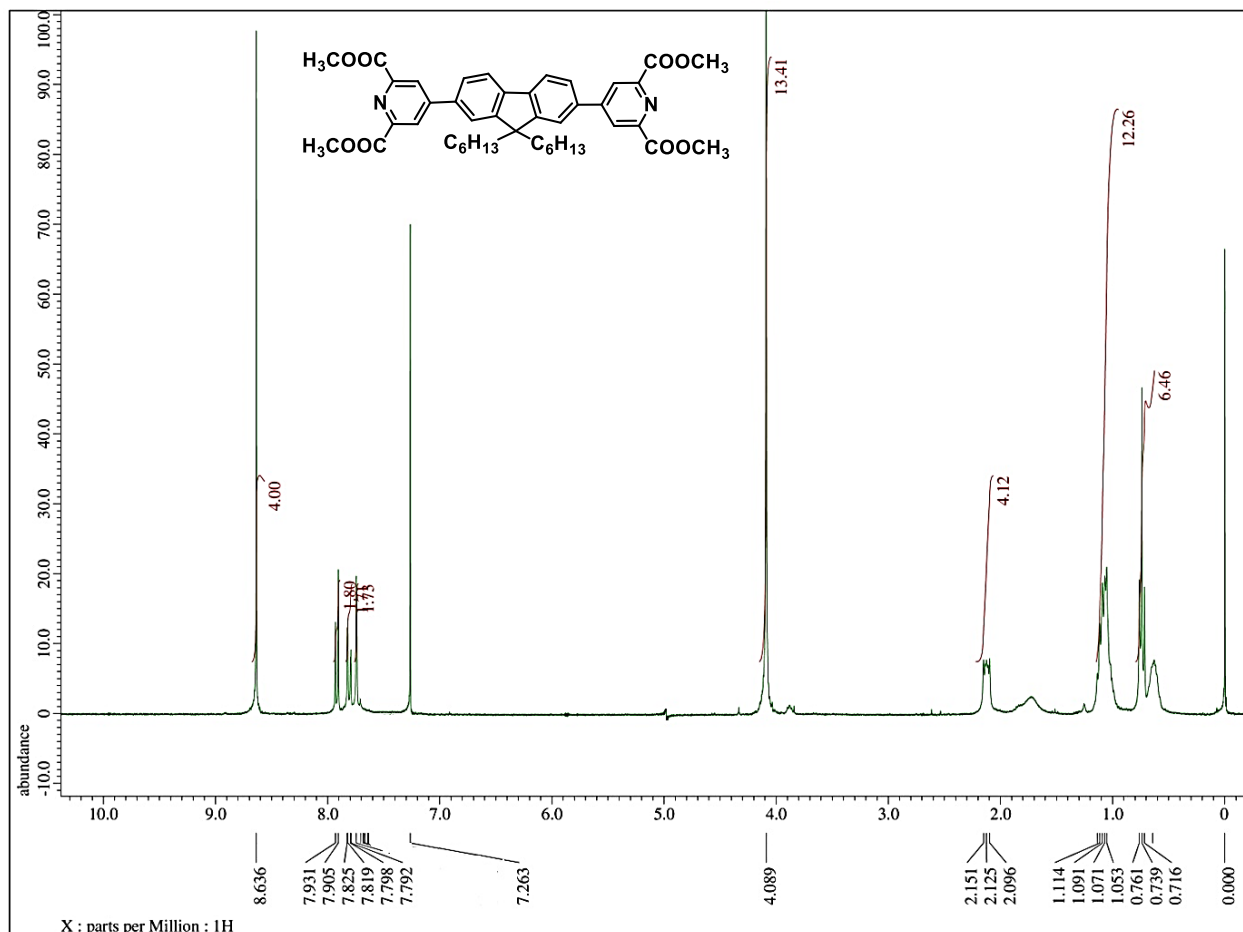


Figure S1. ^1H NMR spectrum of compound 3.

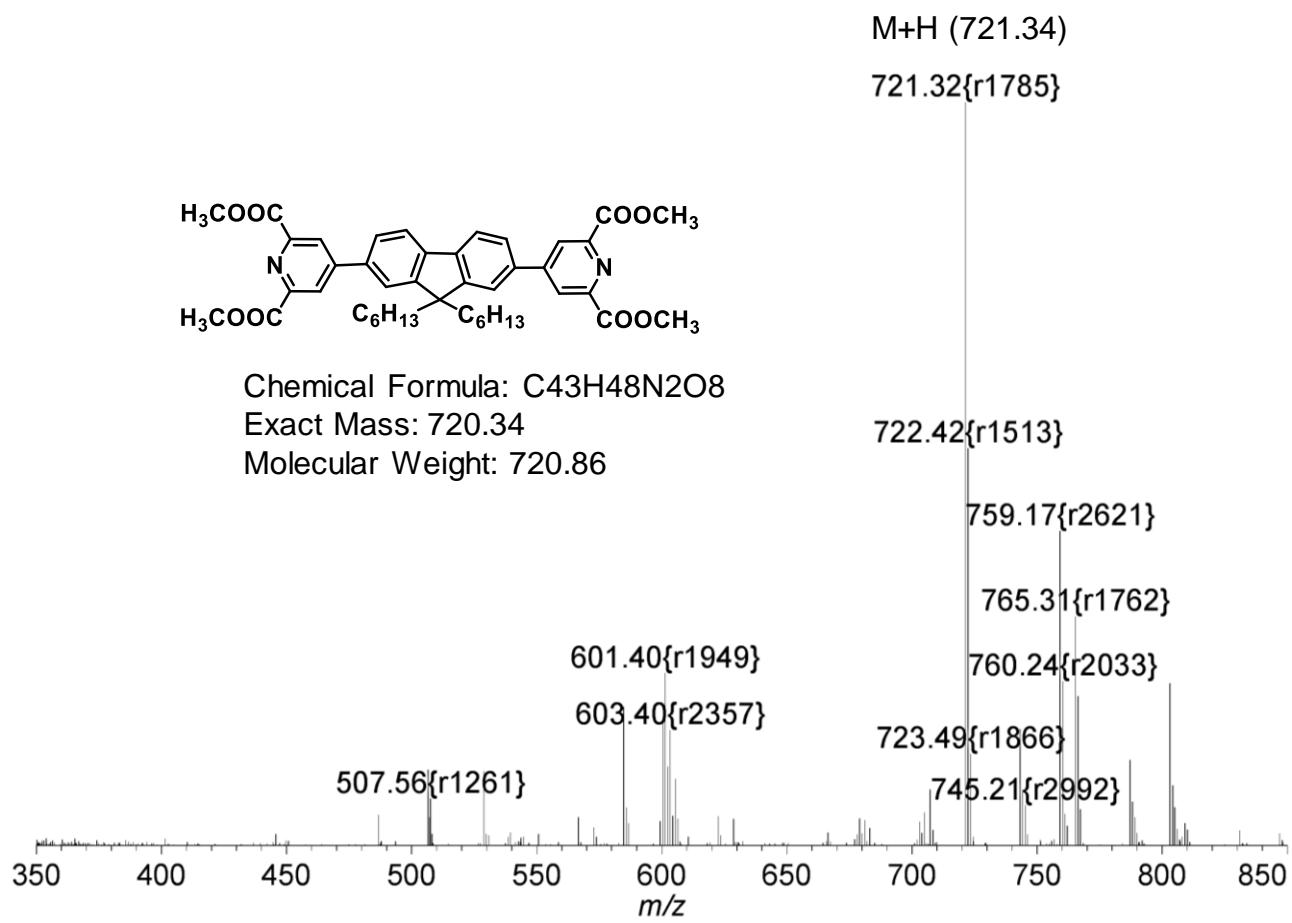


Figure S2. MALDI-TOF spectrum of compound 3.

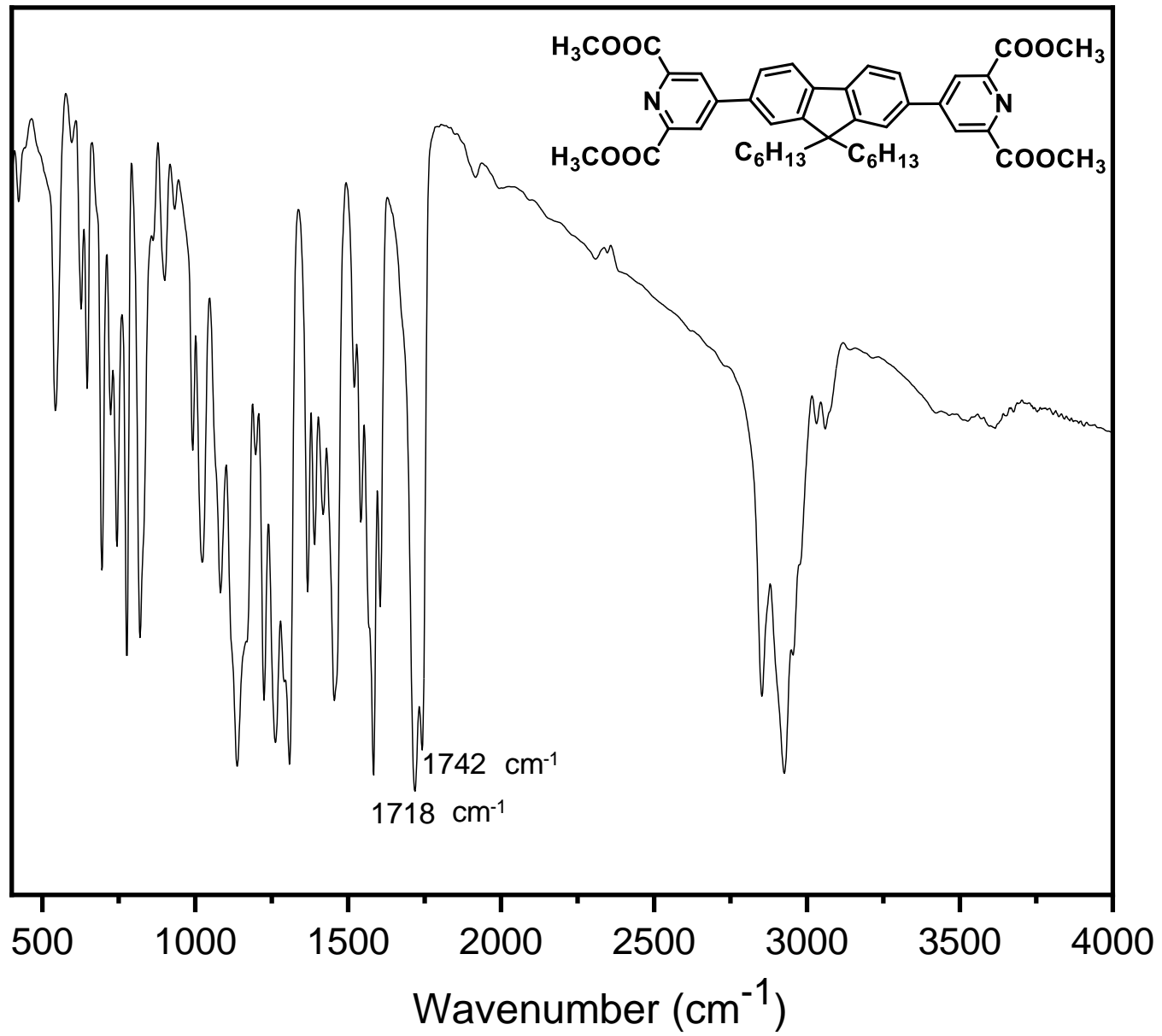


Figure S3. FT-IR spectrum of compound 3 (1742 and 1718 C=O stretching frequencies in COOCH_3 group).

2. ^1H NMR, MALDI-TOF and FT-IR spectra of ligand (L)

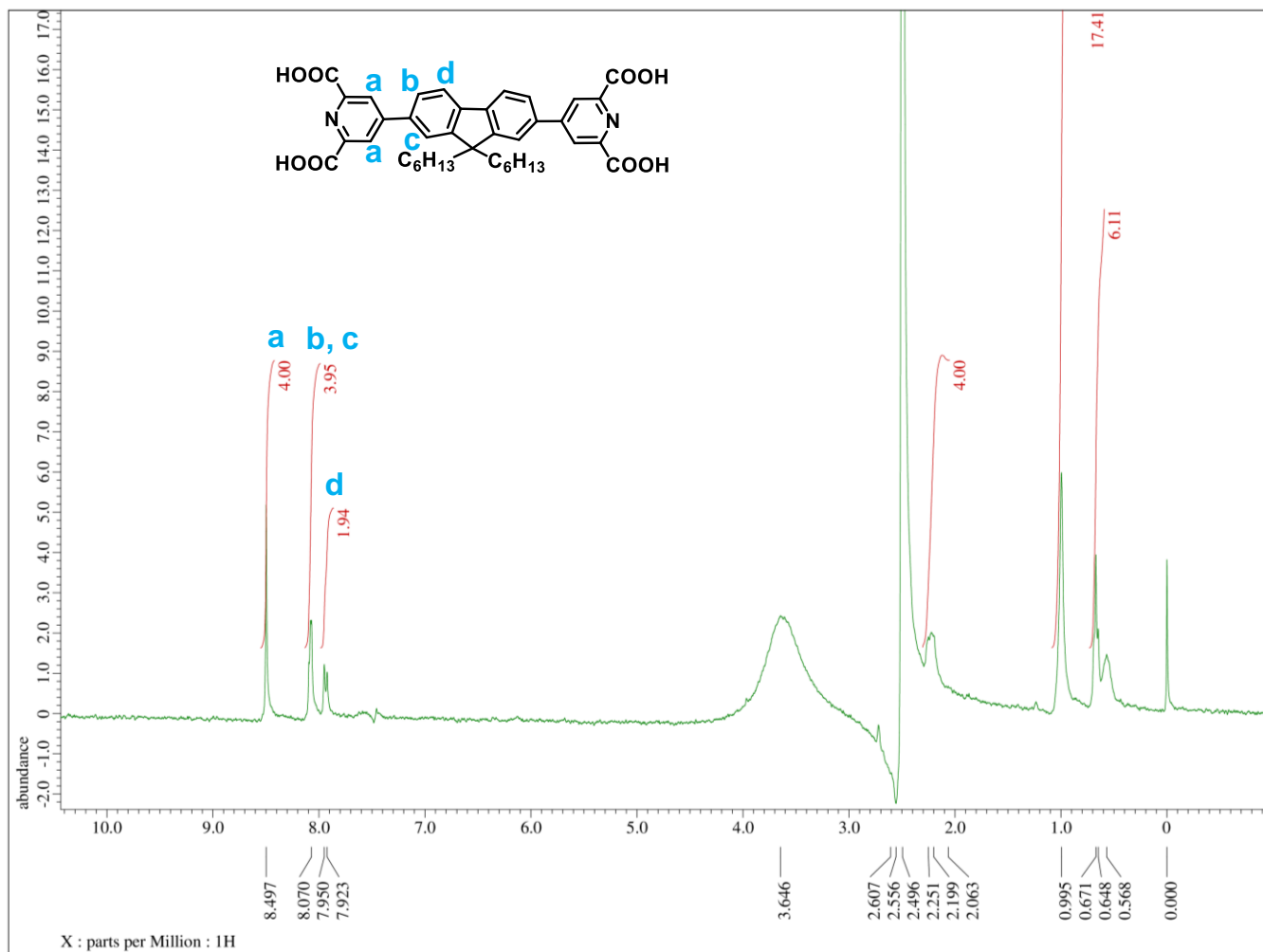


Figure S4. ^1H NMR spectrum of L.

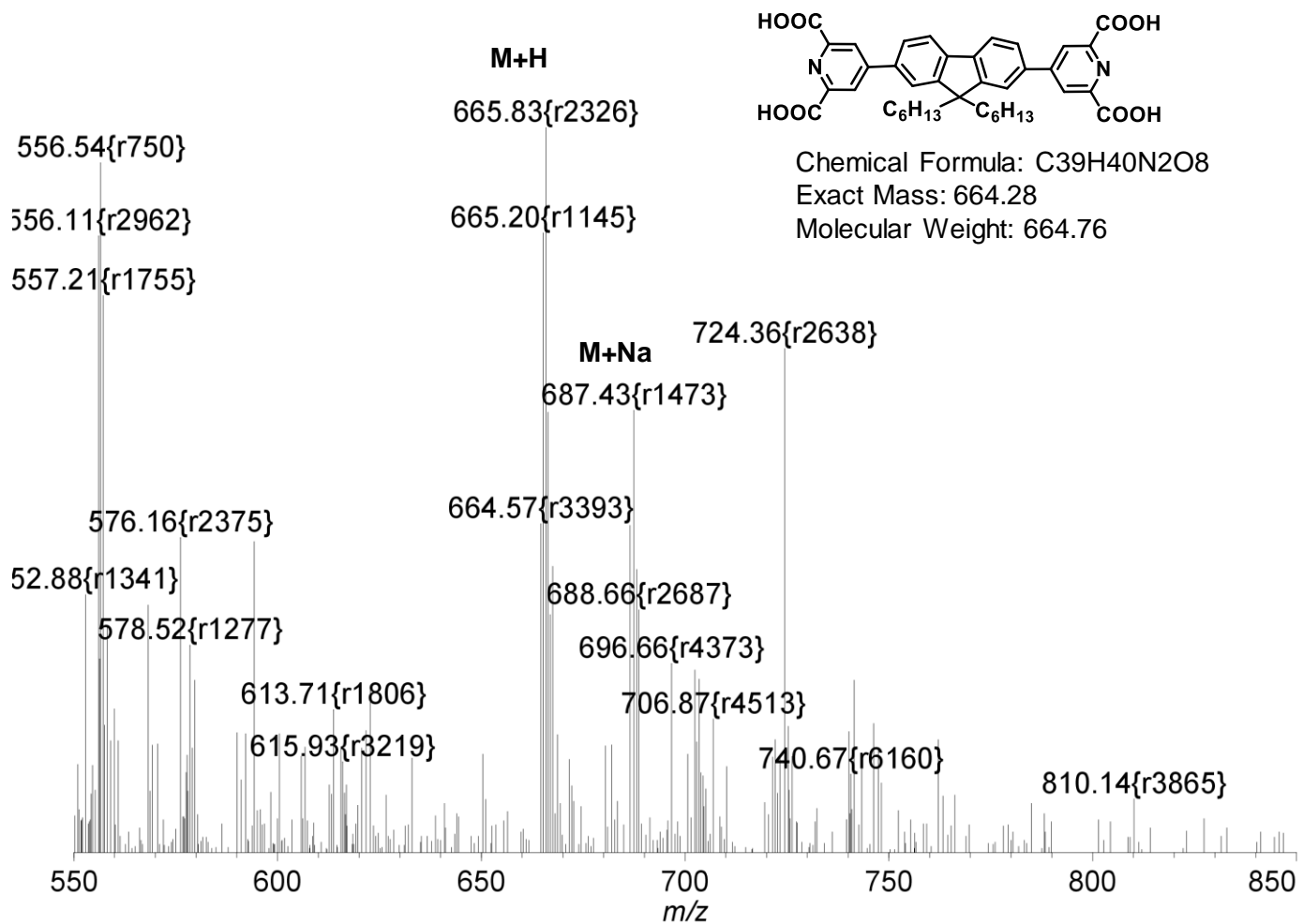


Figure S5. MALDI-TOF spectrum of L.

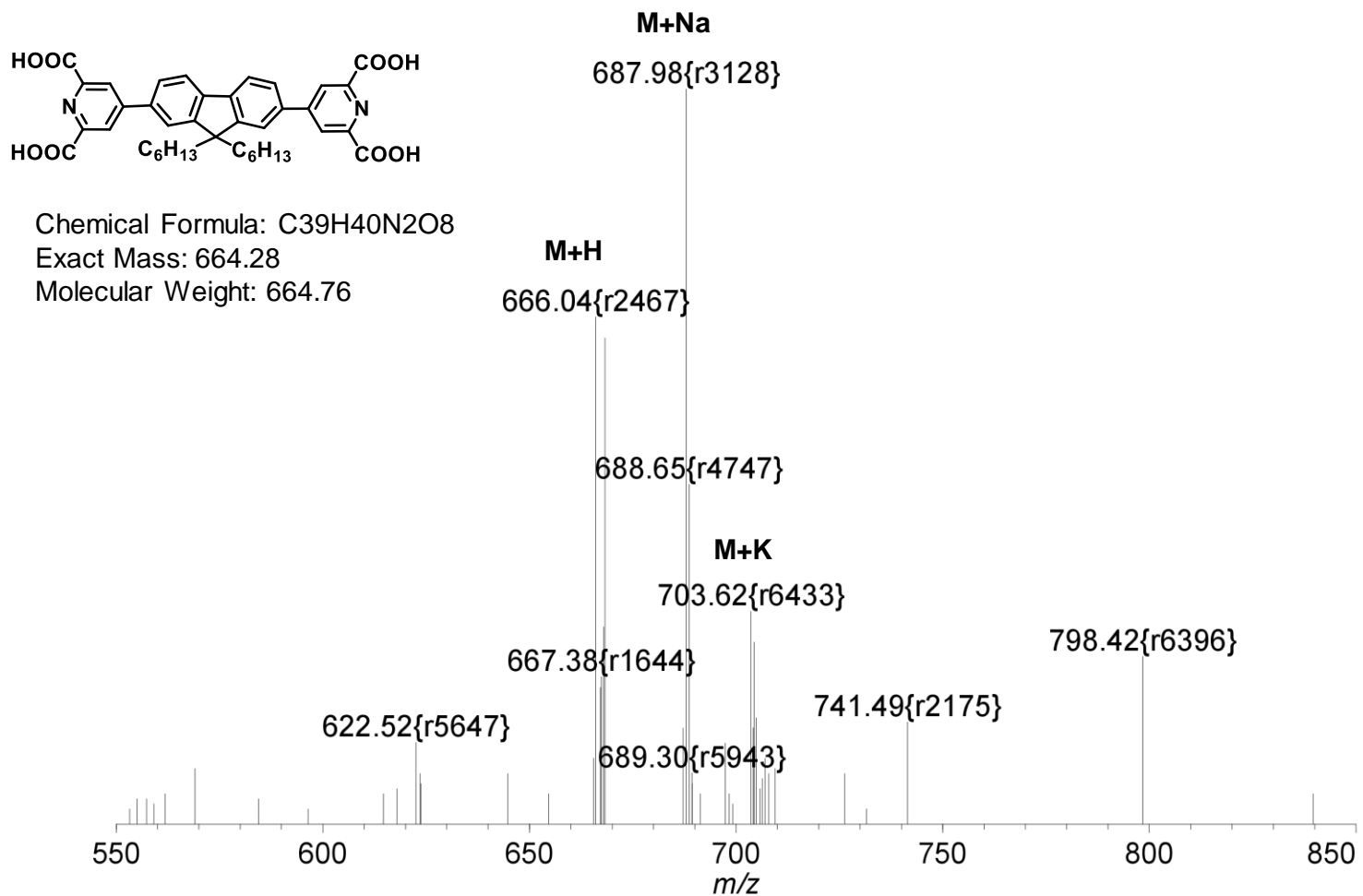


Figure S6. MALDI-TOF spectrum of L.

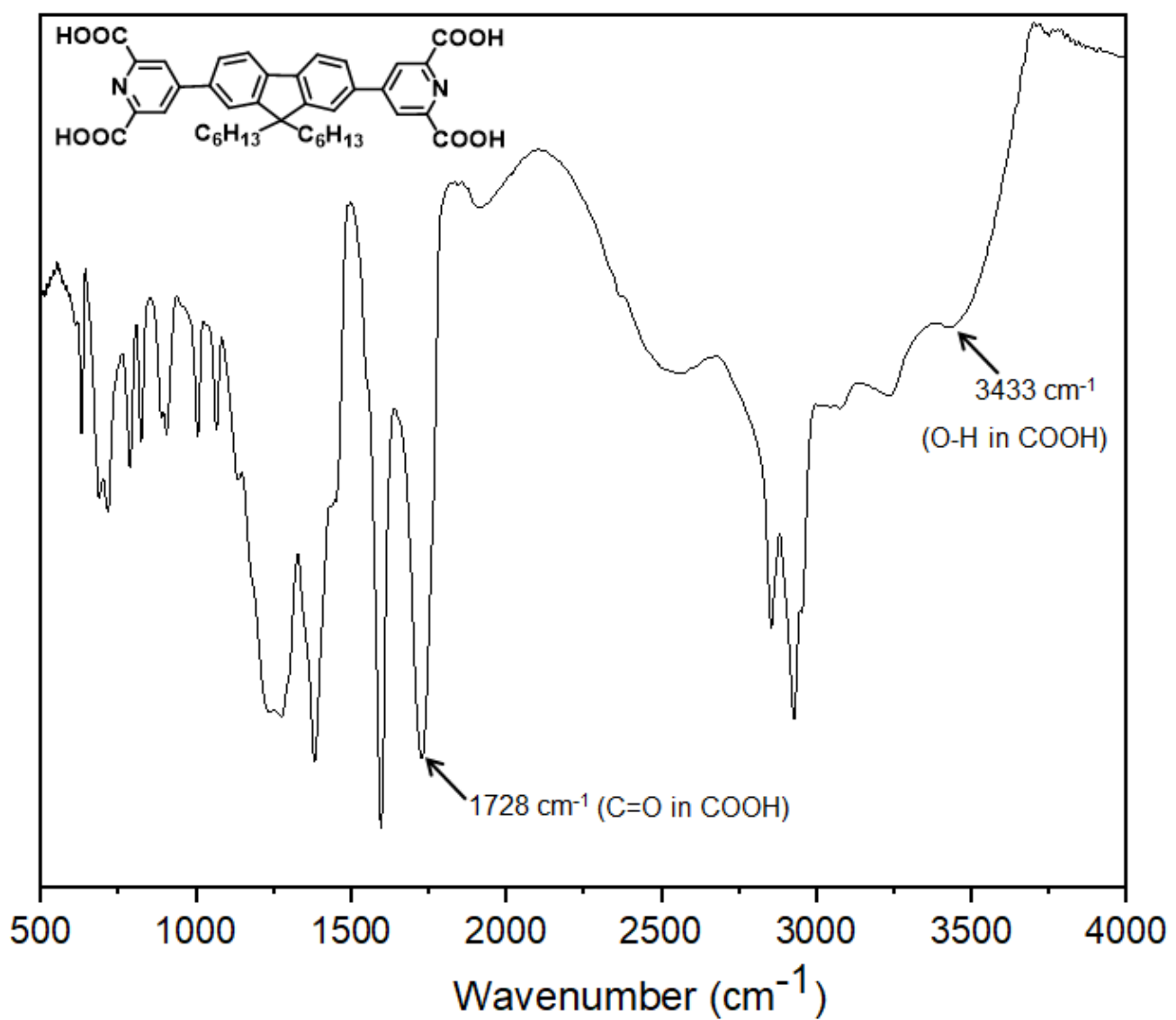
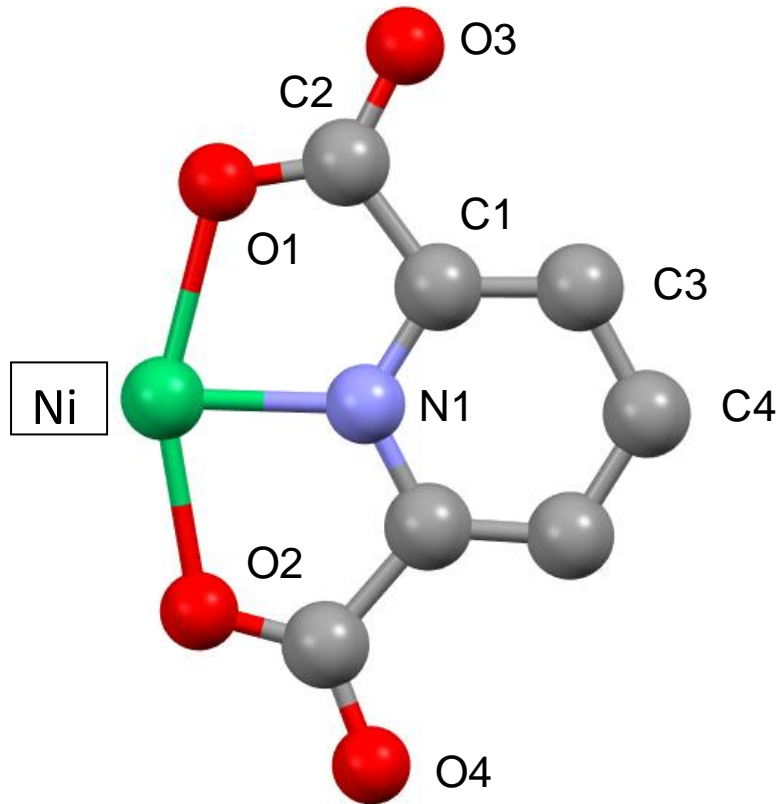


Figure S7. FT-IR spectrum of L.

3. XANFS Data of polyNi

Table S1. The coordination lengths around the Ni ion in polyNi



R -factor: 1.7%	N	$R / \text{\AA}$	R_{eff}	Δ
N1	2	2.071	1.965	0.1066
O1	2	2.214	2.096	0.1186
O2	2	2.204	2.183	0.0205
C1	4	2.834	2.859	-0.0251
C2	4	2.916	2.893	0.0238
O3	3	4.017	4.096	-0.0782
O4	1	4.280	4.162	0.1177
C3	4	4.247	4.212	0.0345
C4	2	4.631	4.623	0.0013

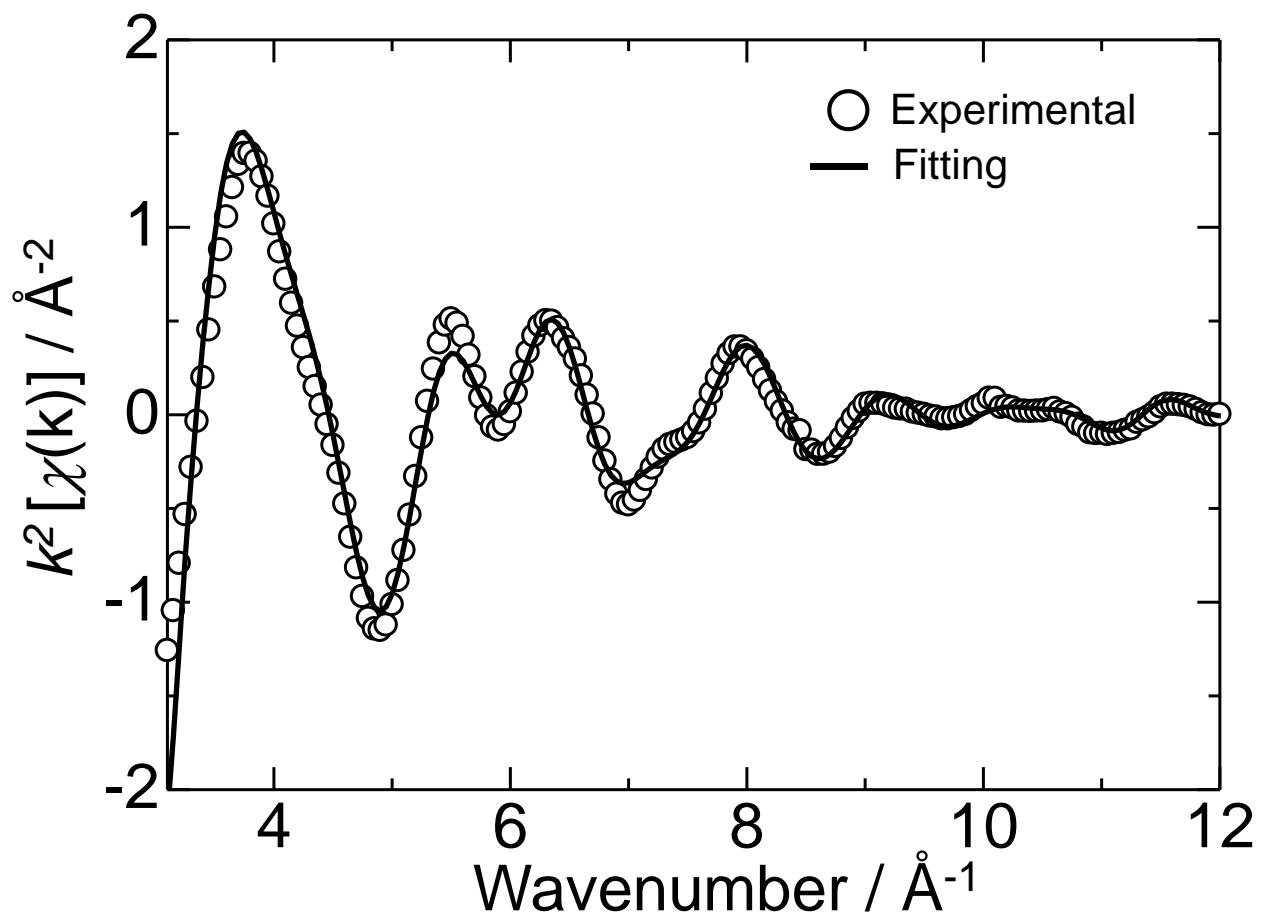


Figure S8. EXAFS oscillation of **polyNi**.

4. XPS data of polyNi

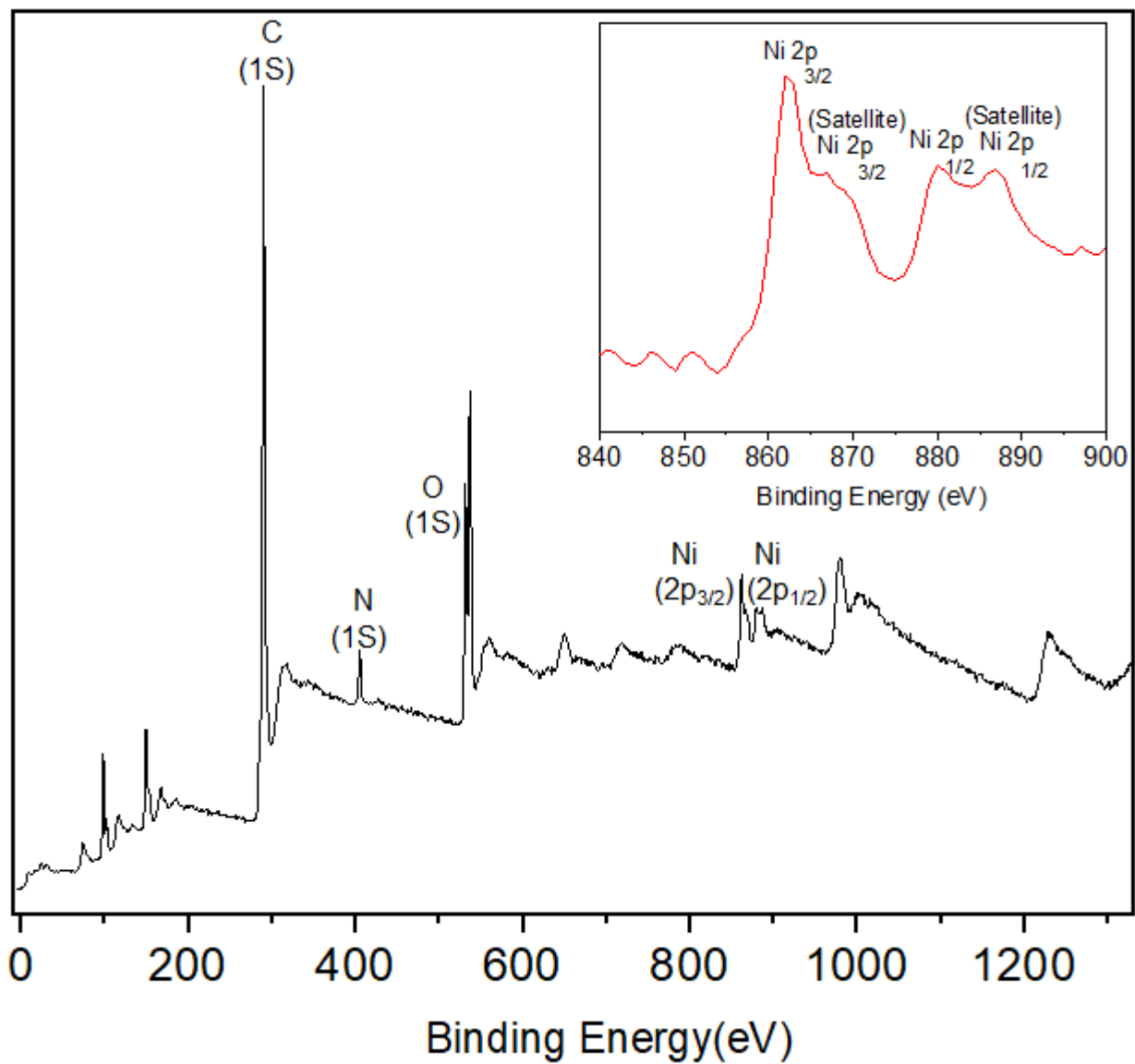


Figure S9. XPS data of polyNi.

5. Derivative TG plot of polyNi-Im

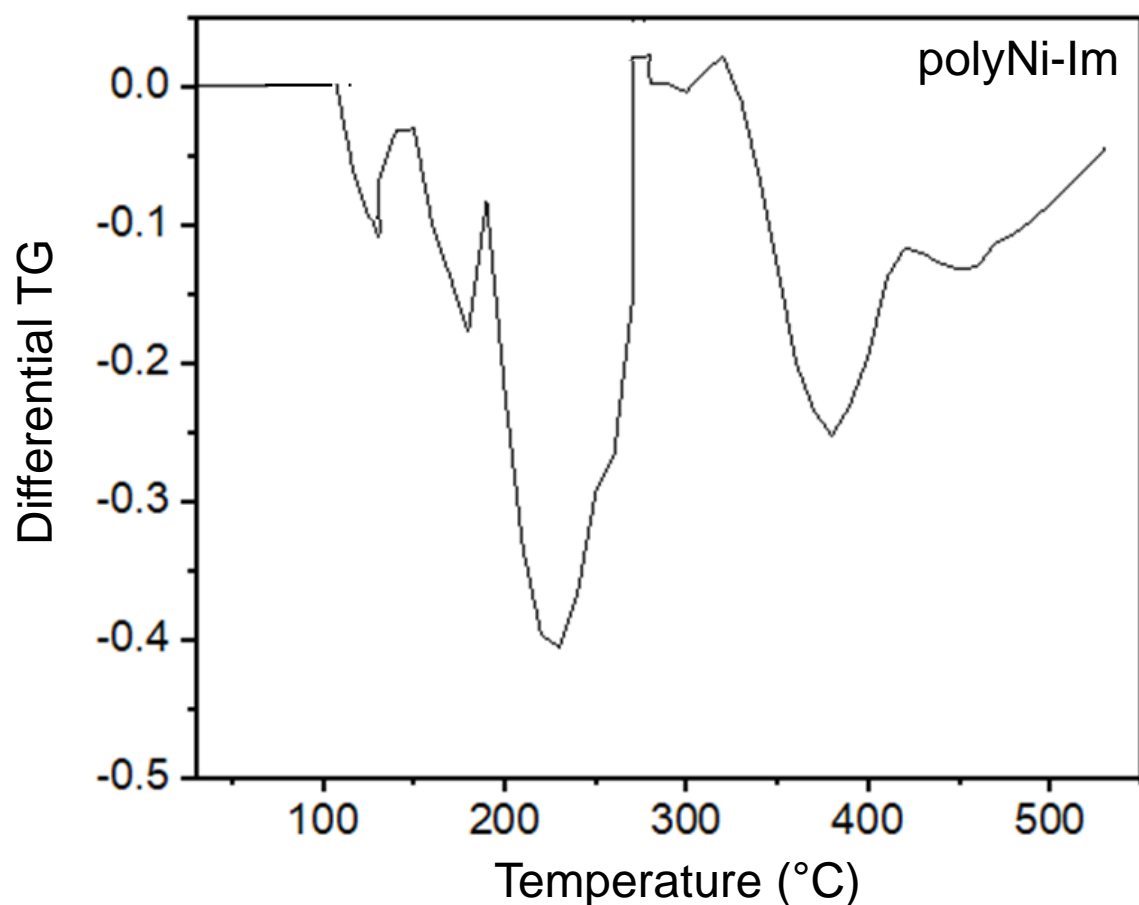


Figure S10. Derivative TG plot of **polyNi-Im**.

6. FT-IR analysis of imidazole, polyNi, and polyNi-Im

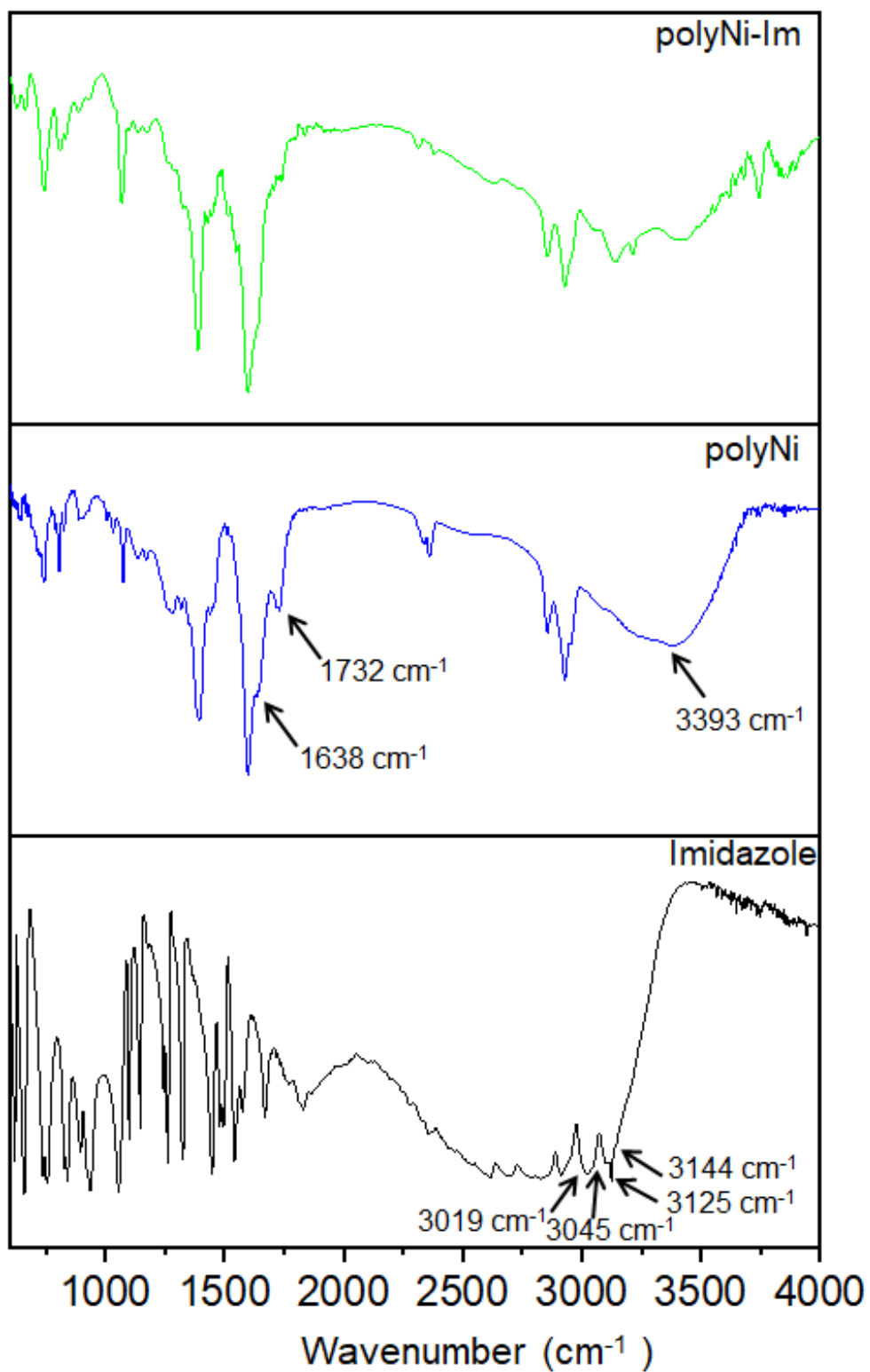


Figure S11. FT-IR spectra of Imidazole, **polyNi**, and **polyNi-Im**.

7. MALDI-TOF analysis of polyNi and polyNi-Im

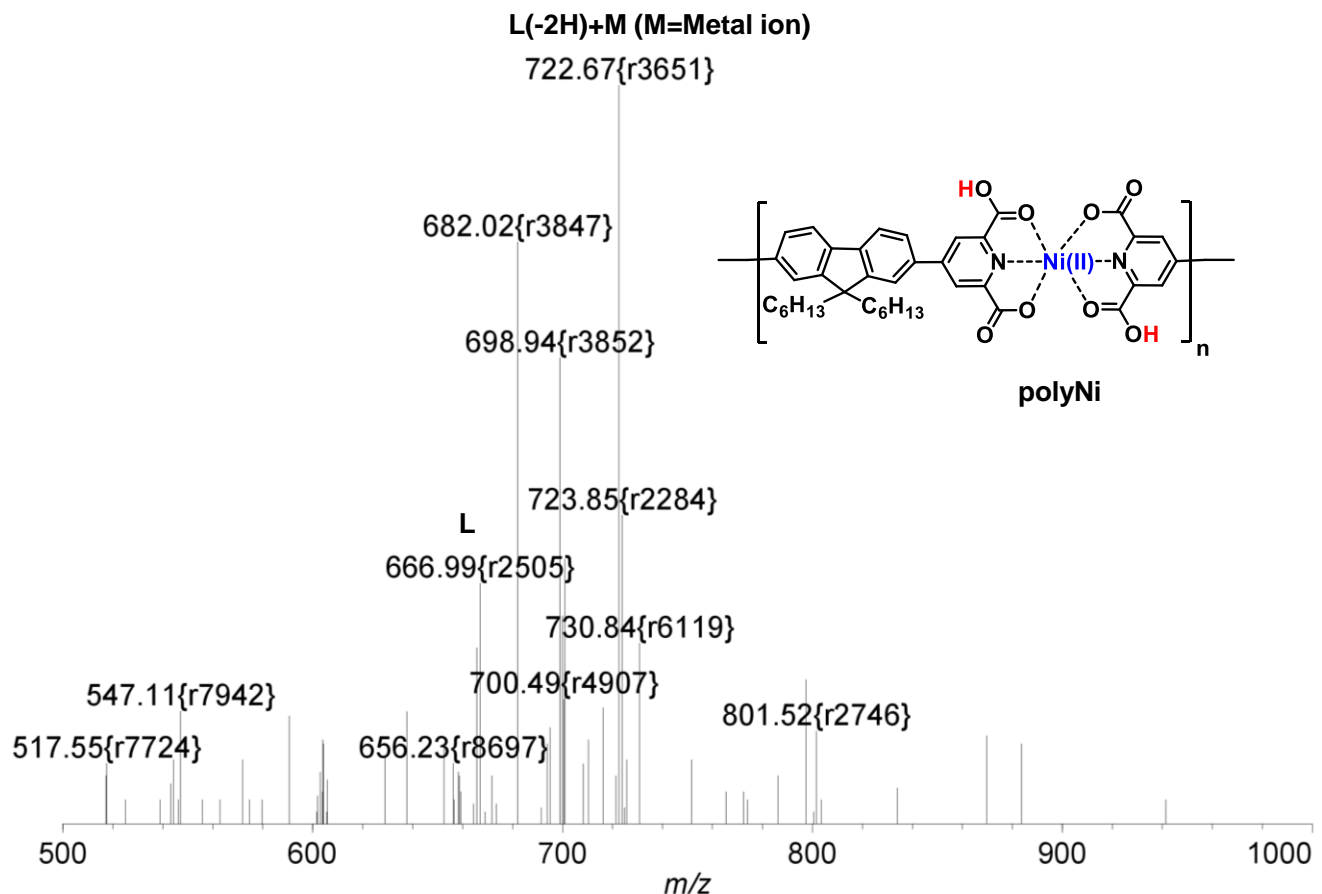


Figure S12. MALDI-TOF spectrum of polyNi.

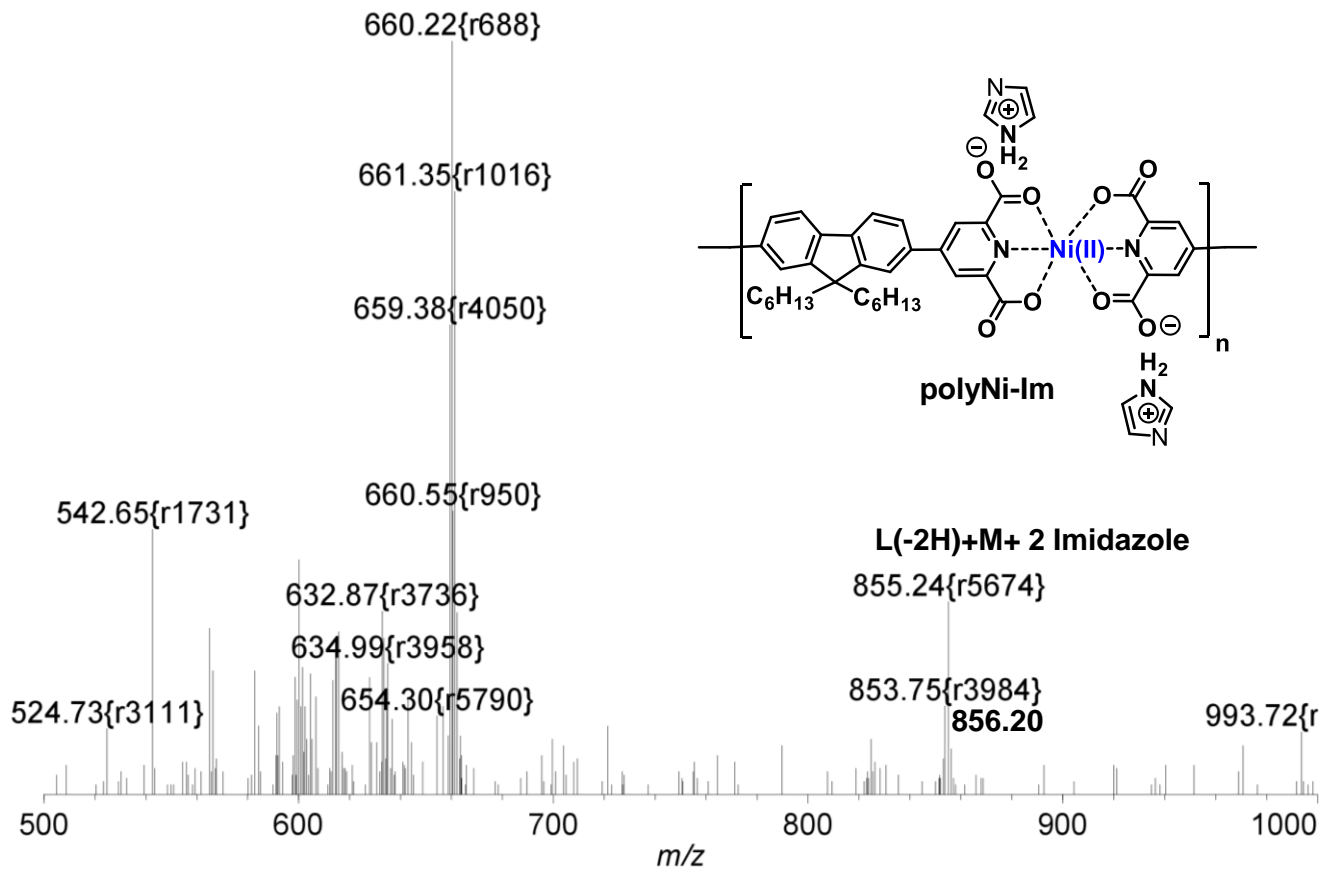


Figure S13. MALDI-TOF spectrum of **polyNi-Im**.

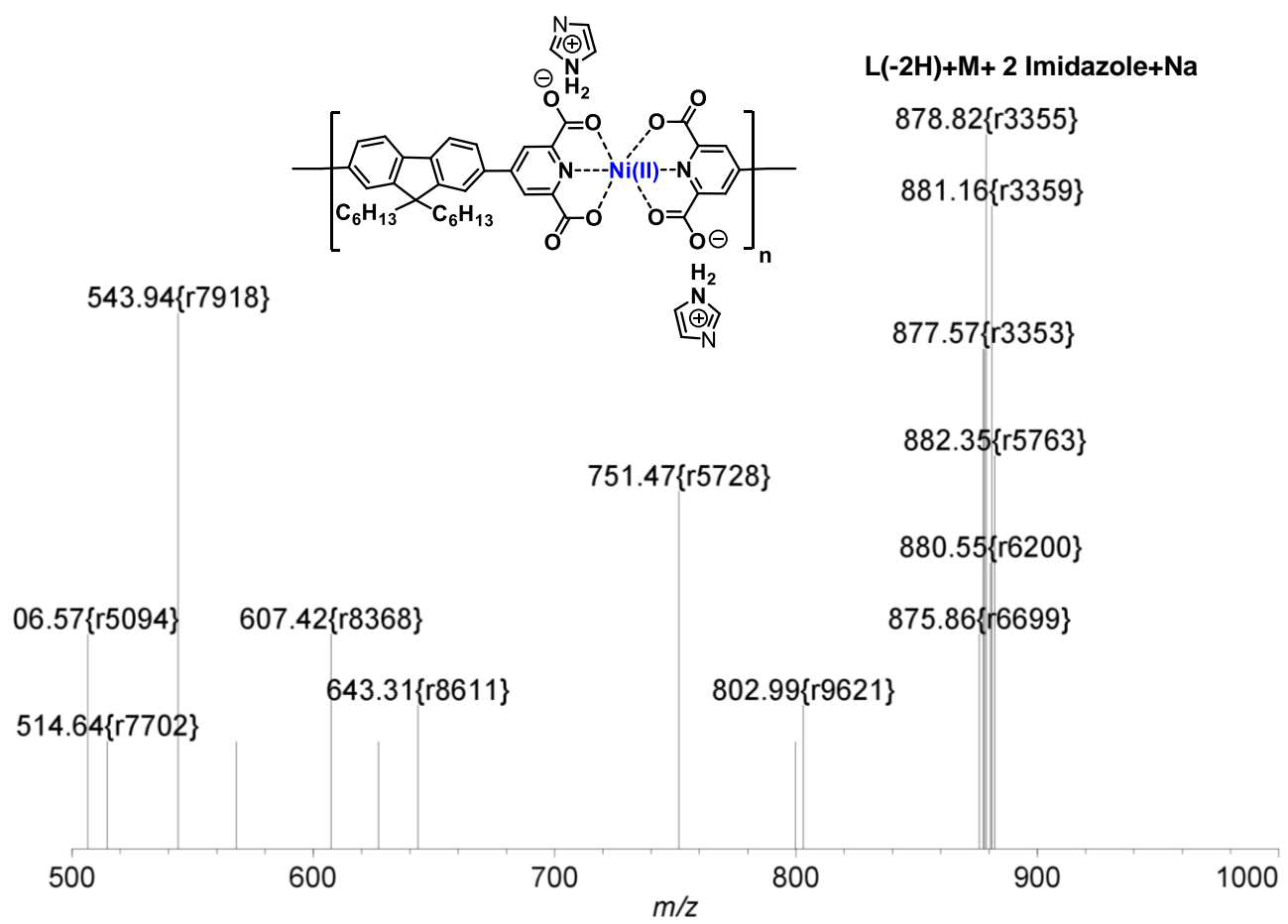


Figure S14. MALDI-TOF spectrum of **polyNi-Im**.

8. SEM images of polyNi and polyNi-Im

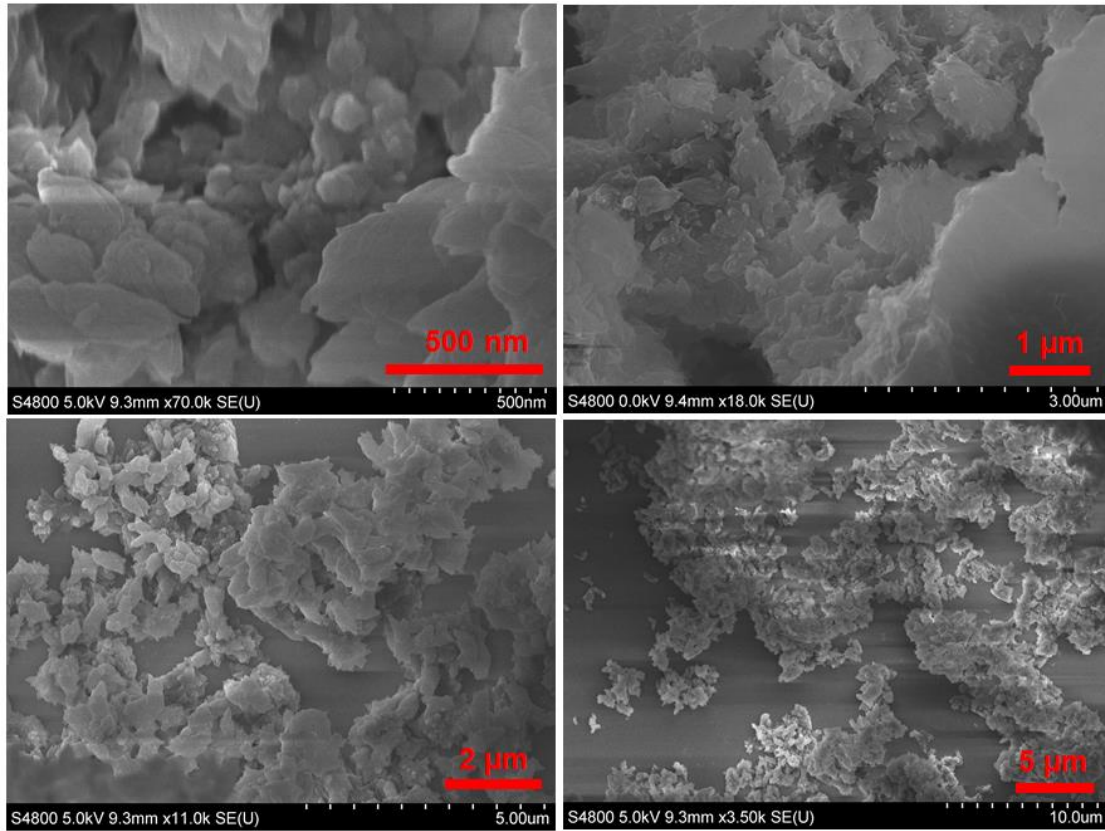


Figure S15. SEM images of **polyNi** in various magnifications.

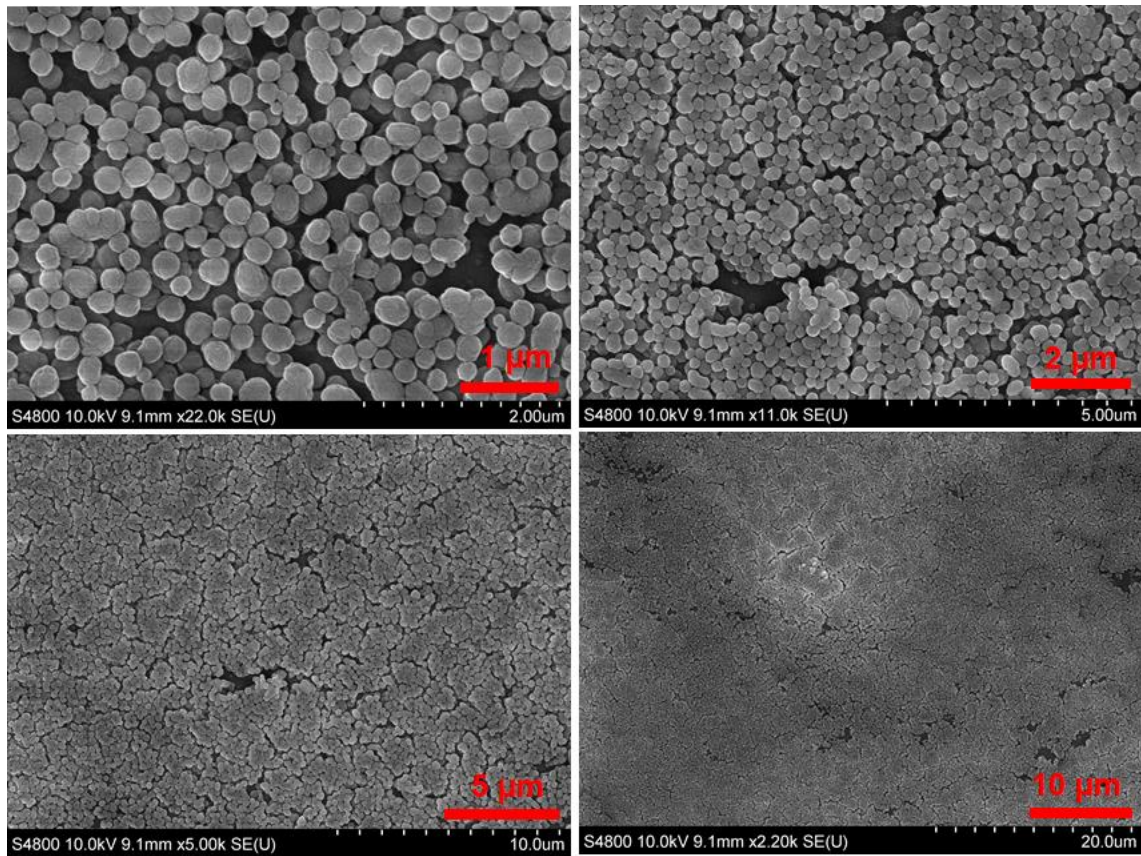


Figure S16. SEM images of **polyNi-Im** in various magnifications.

9. FESEM-EDX analysis of polyNi and polyNi-Im powder and the assembled states

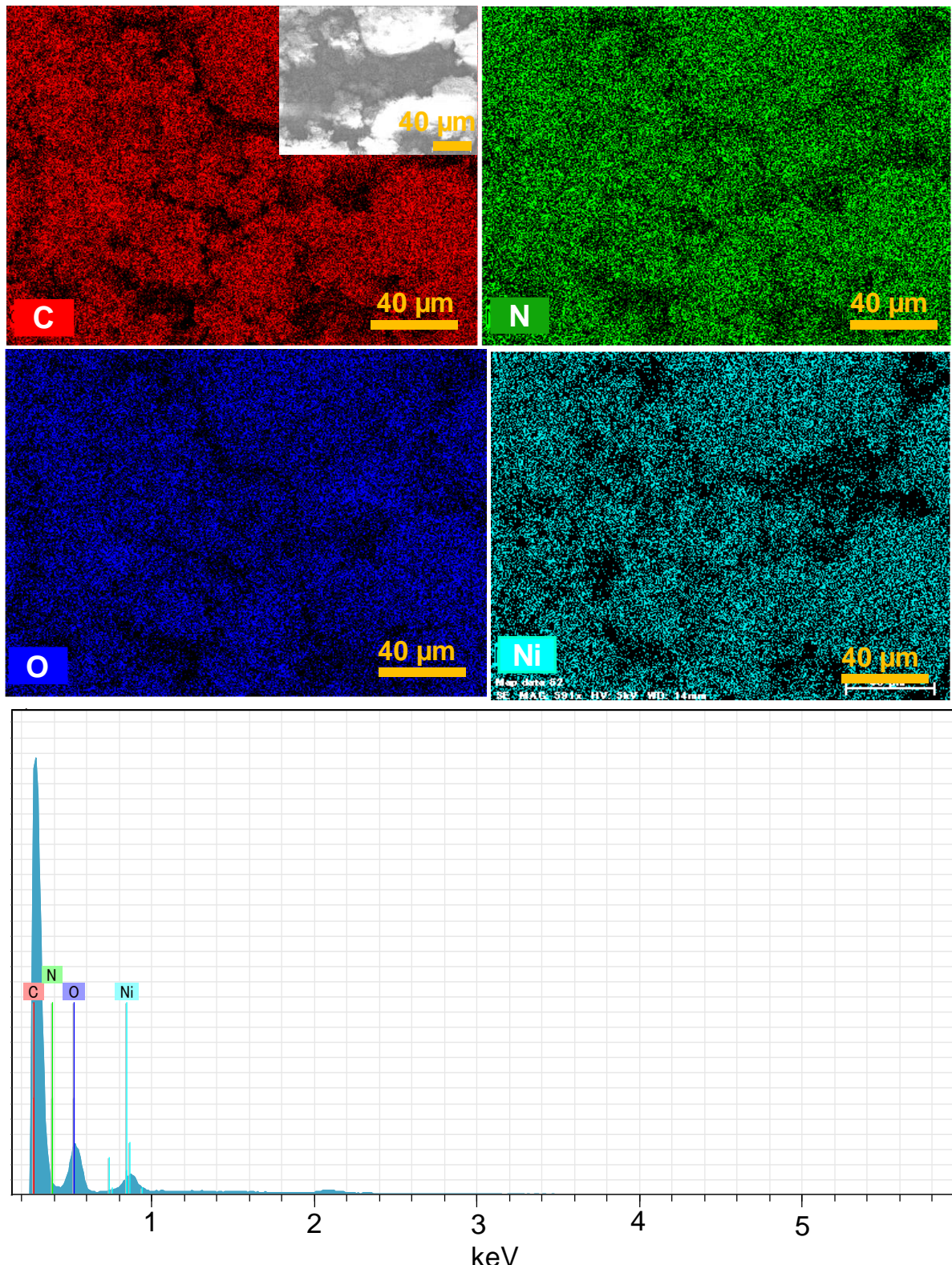


Figure S17. FESEM-EDX elemental mapping and its corresponding spectra of **polyNi** powder sample.

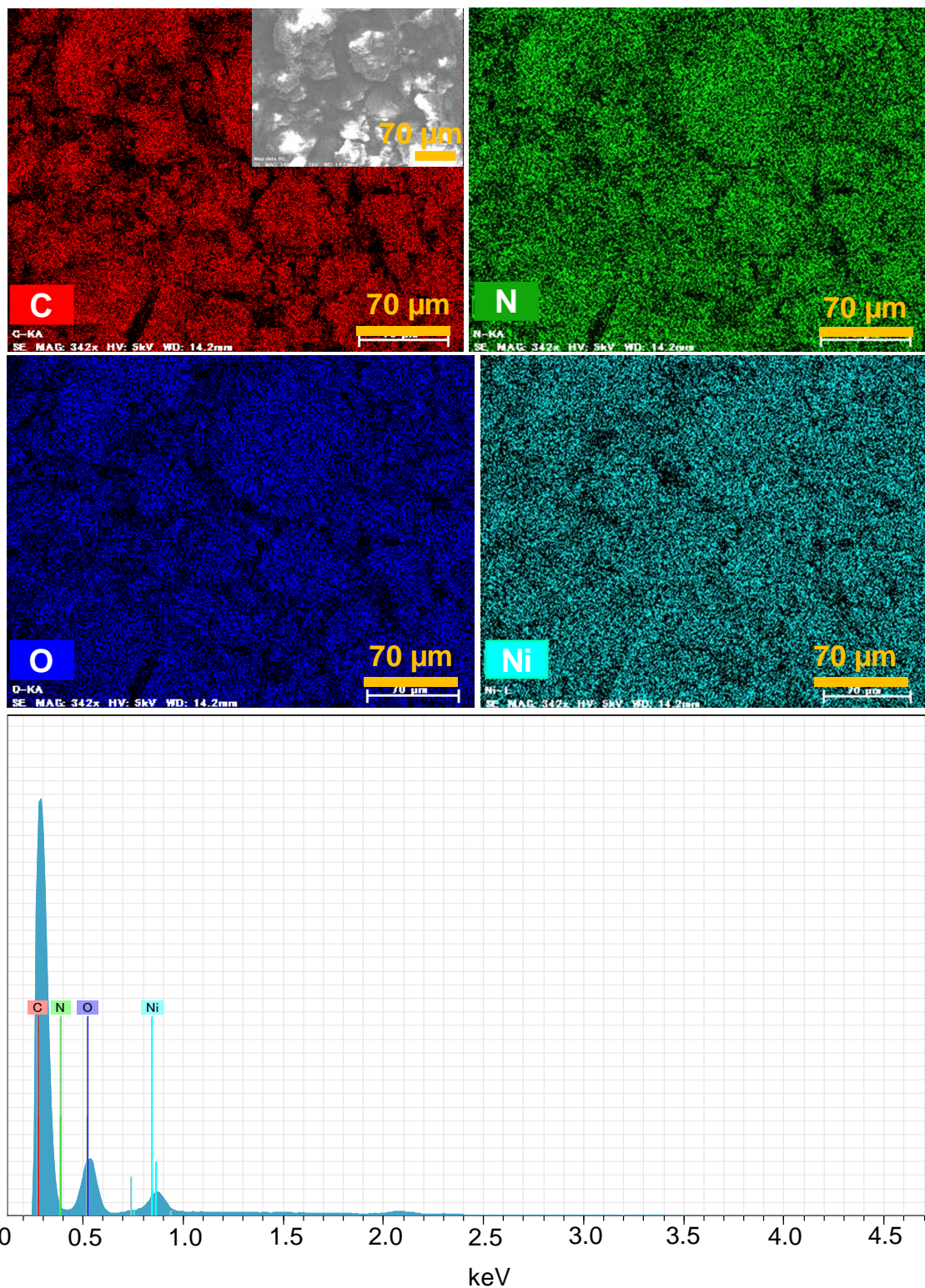


Figure S18. FESEM-EDX elemental mapping and its corresponding spectra of **polyNi-Im** powder sample.

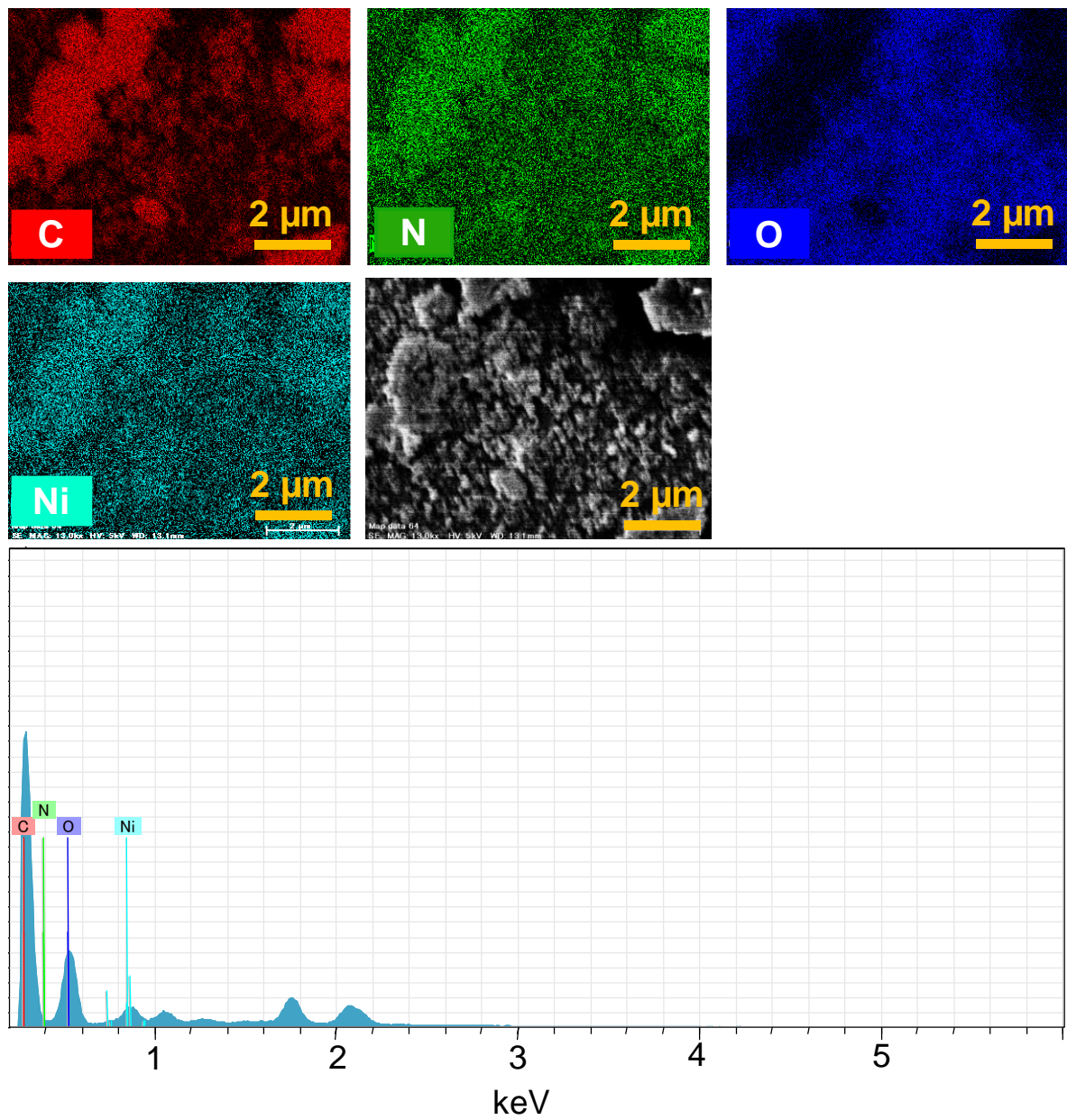


Figure S19. FESEM-EDX elemental mapping and its corresponding spectra of **polyNi** assembled structure.

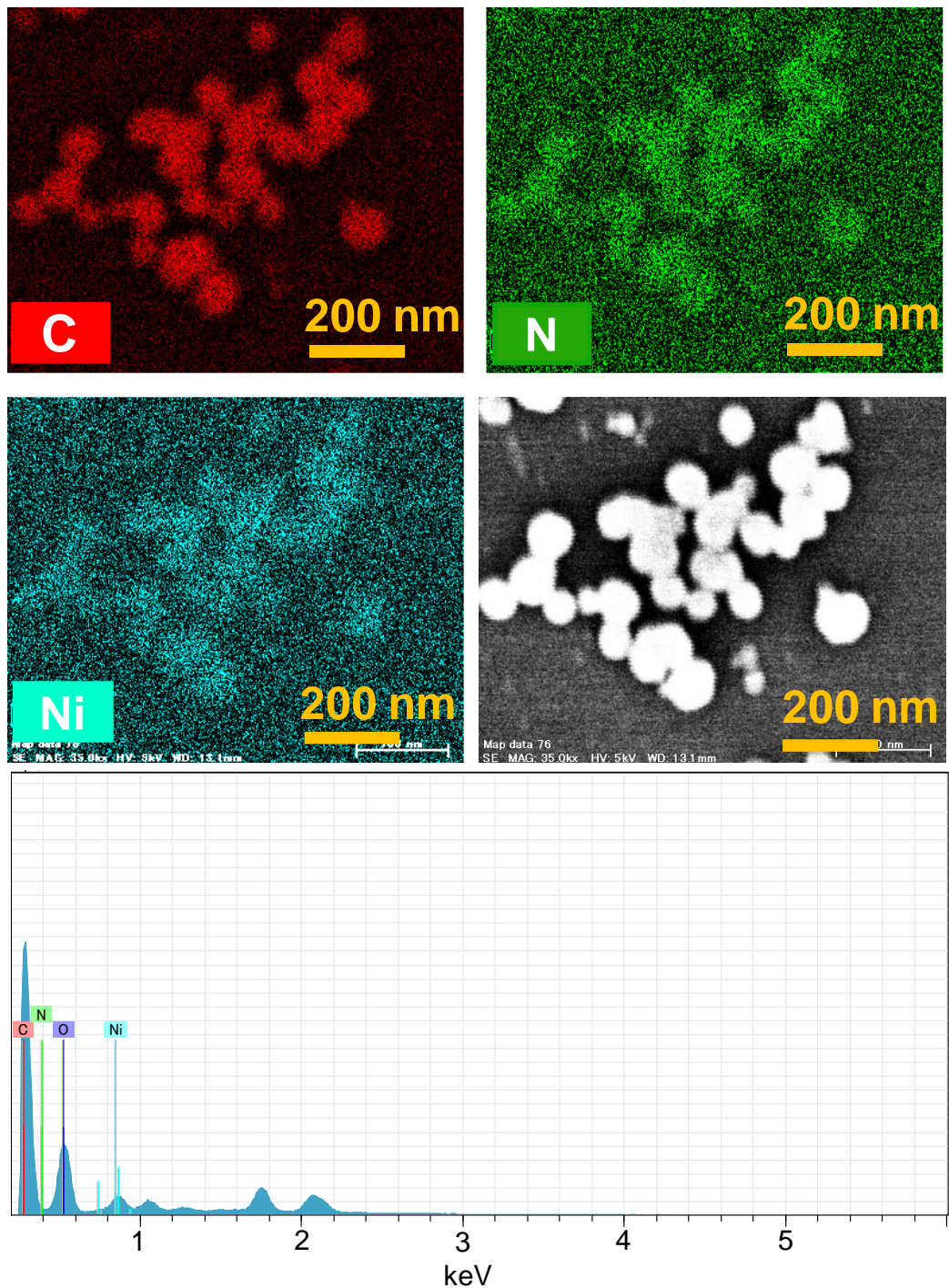


Figure S20. FESEM-EDX elemental mapping and its corresponding spectra of **polyNi-Im** assembled structure.

10. Proton conductivity data of polyNi under anhydrous conditions

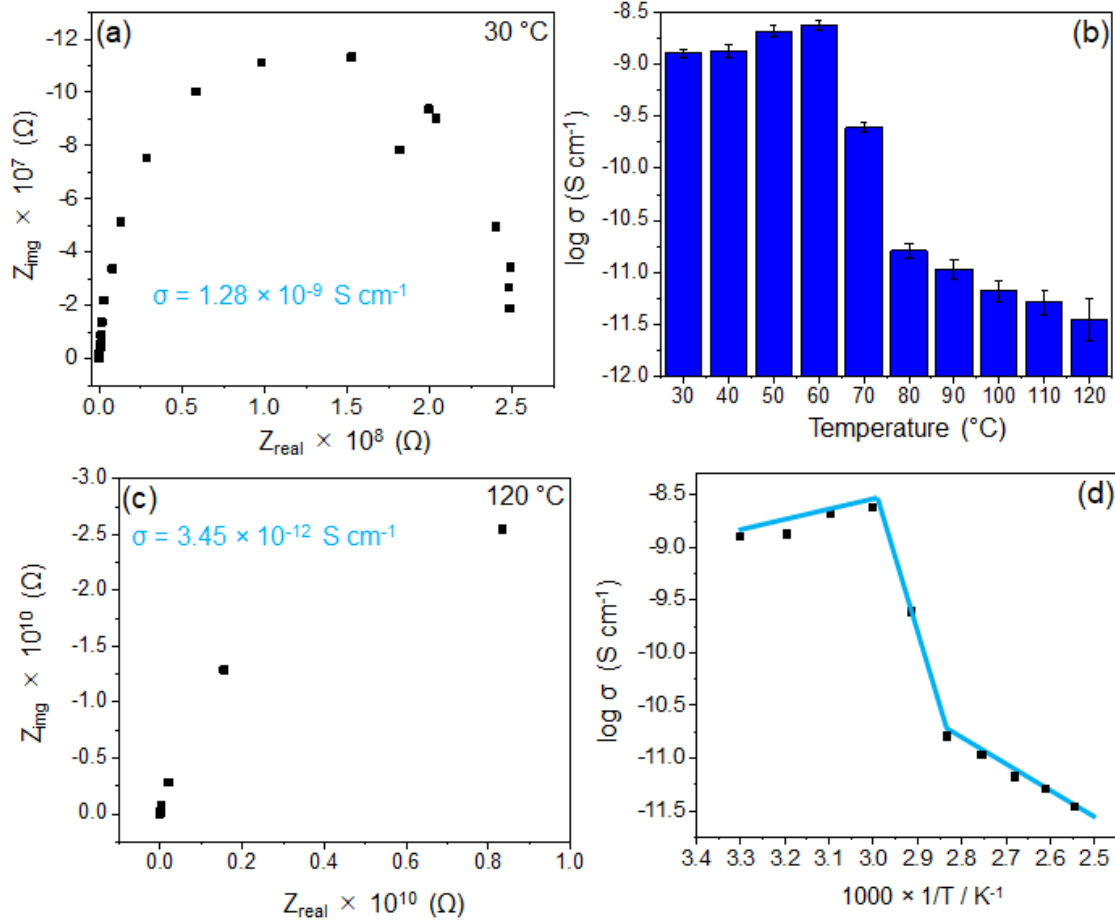


Figure S21. (a) Nyquist diagrams for **polyNi** at different temperatures in anhydrous conditions (b) Bar diagram of conductivities of **polyNi** at different temperatures. (c) Nyquist plot of **polyNi** at 120 °C for proton conduction (d) Arrhenius plot for activation energy measurement for **polyNi**.

11. TGA data of polyNi-Im before and after the impedance measurement

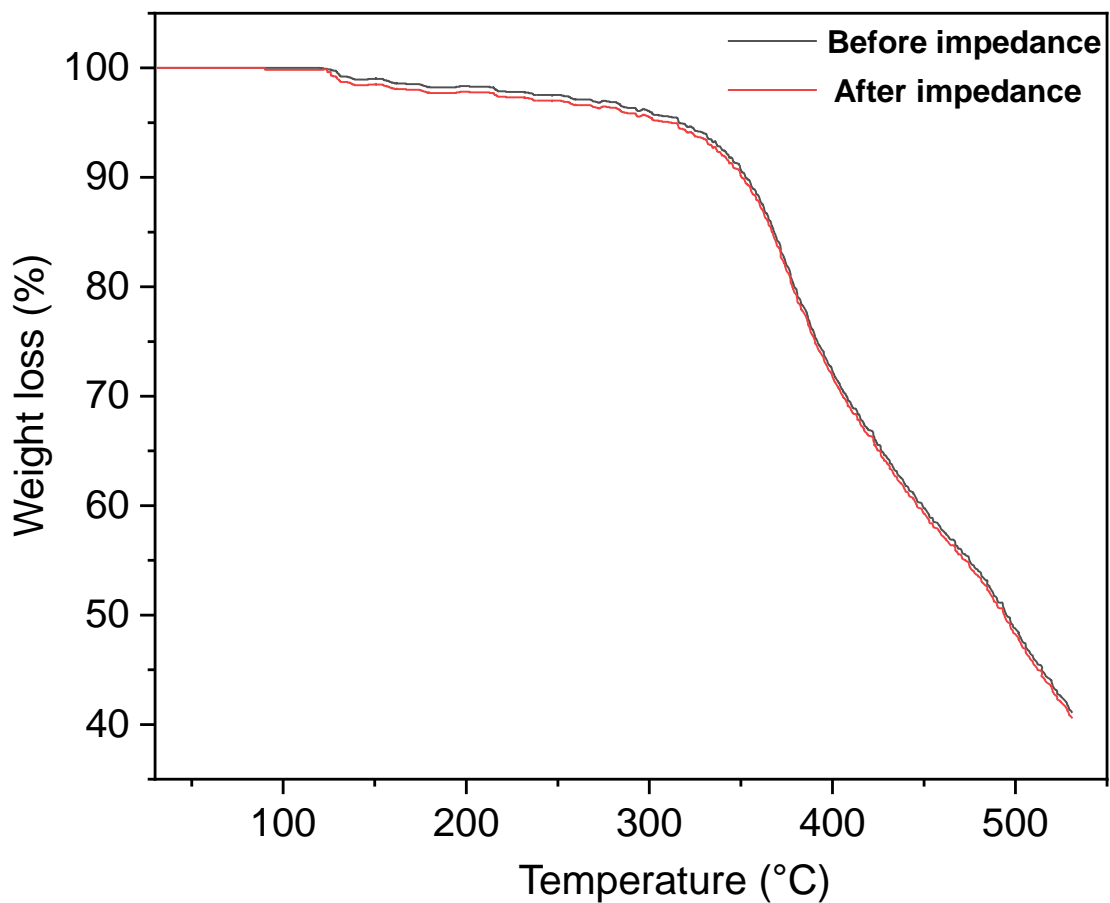


Figure S22. TGA analysis of **polyNi-Im** before and after the impedance measurement.

12. Powder XRD data of polyNi-Im before and after the impedance measurement

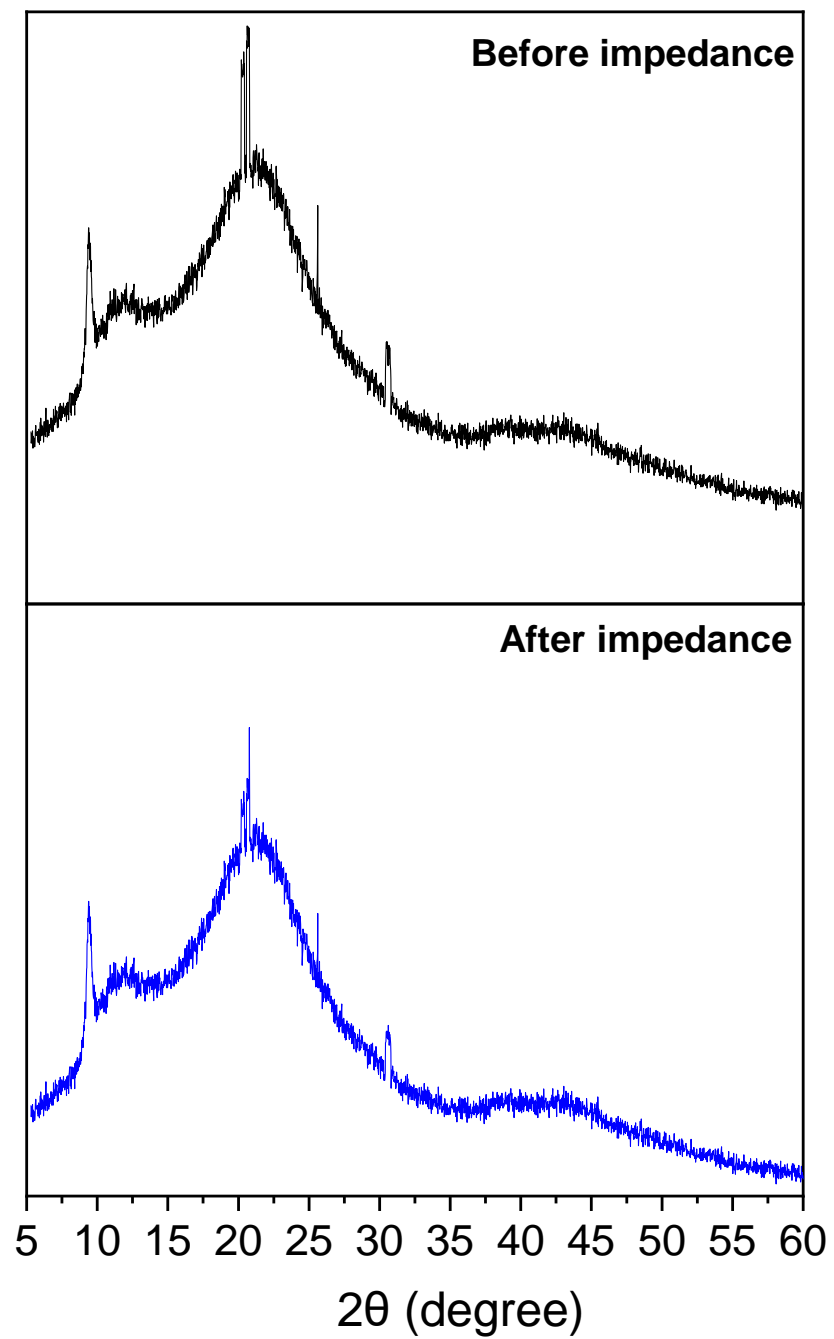


Figure S23. Powder X-ray diffraction data of **polyNi-Im** before and after the impedance measurement.

13. Bode plot of polyNi-Im at 120 °C

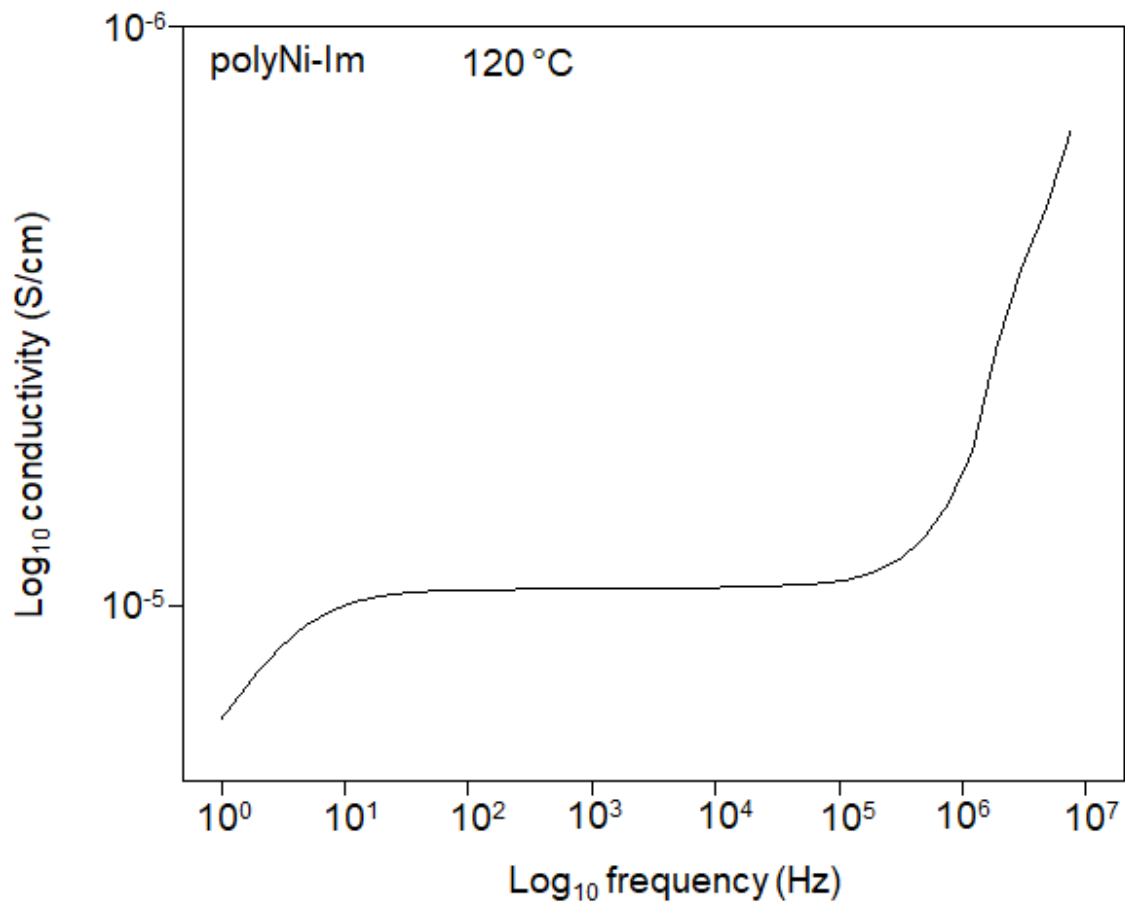


Figure S24. Bode plot of polyNi-Im at 120 °C.

14. Nyquist plot of polyNi-Im at 120 °C

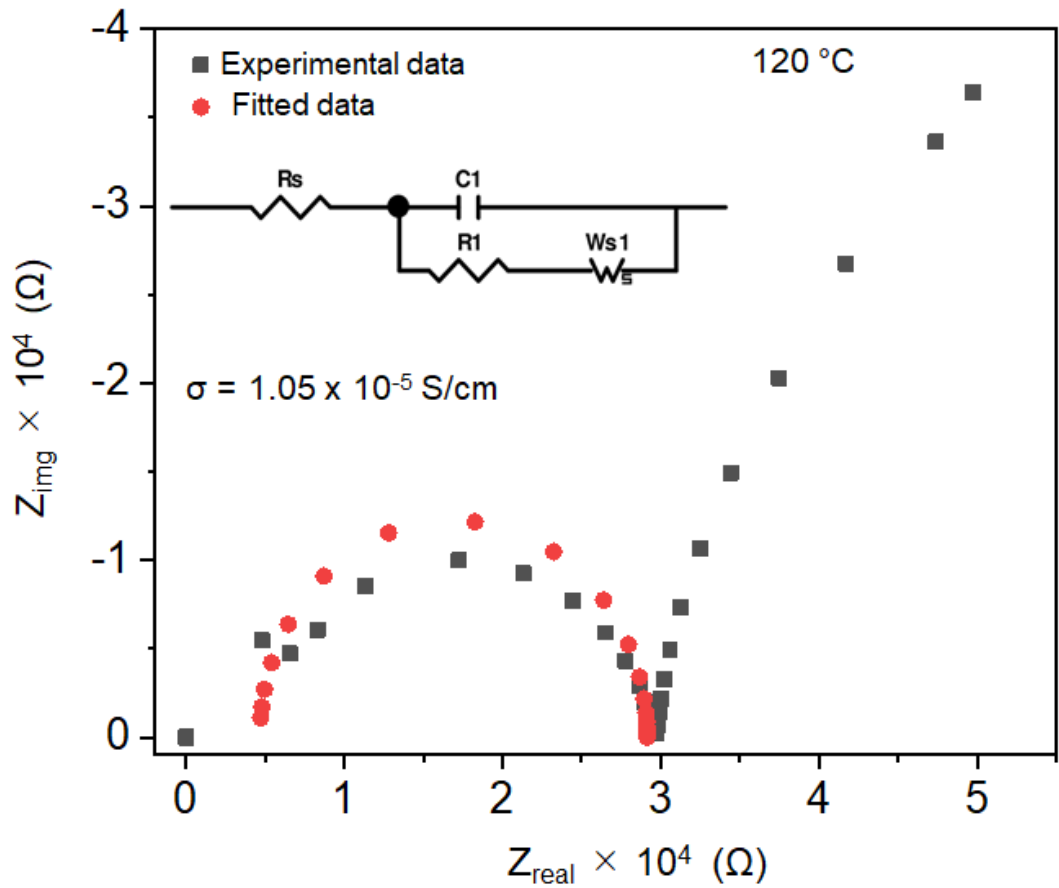


Figure S25. Nyquist plot of polyNi-Im (experimental and fitted data) at 120 °C (inset: An equivalent circuit which is used for the fitting the data).

15. Comparison of proton conductivity of polyNi-Im at 120 °C with different kinds of imidazole loaded materials

Table S2. Comparison of proton conductivity of polyNi-Im at 120 °C with different kinds of imidazole loaded materials.

Compounds	Proton Conductivity at 120 °C (S/cm)	Activation Energy (E_a)	Reference
Im@{Al(μ 2-OH) (1,4-ndc)}n	2.2×10^{-5}	0.60	<i>Nature Mater.</i> 2009 , 8, 831-836.
Im@{Al(μ 2-OH) (1,4-bdc)}n	1.0×10^{-7}	0.90	<i>Nature Mater.</i> 2009 , 8, 831-836.
[Zn3(H2PO4)6(H2O)3] (Hbim)	1.3×10^{-3}	0.50	<i>J. Am. Chem. Soc.</i> 2013 , 135, 11345-11350
imidazole@UiO-67	1.44×10^{-3}	0.36	<i>Dalton Trans.</i> 2015 , 44, 12976-12980
OF \subset Im	2.4×10^{-5}	0.20	<i>Chem. Mater.</i> 2016 , 28, 5847-5854
polyPtC-Im	1.50×10^{-5}	0.41	<i>ACS Appl. Mater. Interfaces</i> 2017 , 9, 13406-13414
polyNi-Im	1.05×10^{-5}	0.45	This work